JCB Journal of Cell Biology

ARTICLE

PAK2 links cell survival to mechanotransduction and metabolism

Hannah K. Campbell[1], Alicia M. Salvi[1], Timothy O'Brien[2], Richard Superfine[2], and Kris A. DeMali[1]

Too little or too much force can trigger cell death, yet factors that ensure the survival of cells remain largely unknown. Here, we demonstrate that E-cadherin responds to force by recruiting and activating p21-activated protein kinase 2 (PAK2) to allow cells to stiffen, metabolize, and survive. Interestingly, PAK2 activation and its control of the apoptotic response are specific for the amplitude of force applied. Specifically, under low amplitudes of physiological force, PAK2 is protected from proteolysis, thereby ensuring cell survival. In contrast, under higher amplitudes of physiological force, PAK2 is left unprotected and stimulates apoptosis, an effect that is prevented by cleavage-resistant forms of the protein. Finally, we demonstrate that PAK2 protection is conferred by direct binding of AMPK. Thus, PAK2 mediates the survival of cells under force. These findings reveal an unexpected paradigm for how mechanotransduction, metabolism, and cell survival are linked.

Introduction

Cells in all organisms from bacteria to eukaryotes are subject to a myriad of forces, such as stretching, compaction, tension, and shear stress. How cells respond to these forces dictates survival, with imbalances in this process leading to cell death. This phenomenon is well characterized in a number of physiological settings. Restricting the flow of air into the lungs (as frequently occurs in patients with severe asthma) triggers epithelial cells lining the airway to apoptose (Cohen et al., 2007). Similarly, too much force on the airway epithelium triggers cell death and lung injury and is a common side effect of patients on ventilators (Wang et al., 2012; Slutsky and Ranieri, 2013; Neto et al., 2016). The association between disruptions in mechanical forces and increased cell death is not limited to epithelial cells. This phenomenon is well characterized in the cardiovascular system. Vessels with disturbed blood flow are predisposed to endothelial cell apoptosis (Li et al., 2005; Huo et al., 2007). Despite the wealth of data suggesting that the amplitude of force impacts cell survival, factors that protect cells under force from cell death are not well described.

External forces are sensed by the cell surface receptors, such as integrins and cadherins. Epithelial cadherin (E-cadherin) binds to E-cadherins on neighboring cells and promotes cell–cell adhesion. In response to force, E-cadherin initiates a signaling cascade that culminates in increased cell stiffening and actomyosin contractility. Several of the signaling components of the signal transduction cascade from E-cadherin to elevated contractility have emerged. In response to force, liver kinase β1 recruits and activates AMP-activated kinase (AMPK; Bays et al., 2017). Active AMPK stimulates Abelson kinase (Abl), which in turn phosphorylates vinculin Y822 (Bays et al., 2017). Once phosphorylated, vinculin promotes RhoA activation and phosphorylation of myosin light chain, ultimately culminating in growth of the cadherin adhesion complex and reinforcement of the actin cytoskeleton-a process known as cell stiffening (Bays et al., 2017). Despite this wealth of information, this pathway is incomplete. Key among the missing pieces is a link between the major regulator of metabolism, AMPK, and the contractility pathway initiated by Abl tyrosine kinase.

Several lines of evidence indicate that the serine/threonine kinase, p21-activated kinase 2 (PAK2), could be a link between AMPK and Abl. First, PAK2 localizes to the cell–cell junctions (Frank et al., 2012) and stimulates the same types of actin-myosin cytoskeletal rearrangements that are necessary for cells to increase contractility (Frank et al., 2012). Second, PAK2 is known to bind, phosphorylate, and activate Abl in vitro (Jung et al., 2008). Third, PAK2 was identified as a potential substrate for AMPK in a chemical screen (Banko et al., 2011). Thus, PAK2 may be an intermediate between AMPK and Abl in the E-cadherin mechanotransduction pathway.

In order for cells to withstand force, it is important that the mechanosignaling pathways also ensure the survival of cells. In addition to being a likely intermediate between AMPK and Abl,

[1]Department of Biochemistry, Roy J. and Lucille A. Carver College of Medicine, University of Iowa, Iowa City, IA; [2]Department of Physics, University of North Carolina, Chapel Hill, NC.

Correspondence to Kris DeMali: kris-demali@uiowa.edu.

© 2019 Campbell et al. This article is distributed under the terms of an Attribution–Noncommercial–Share Alike–No Mirror Sites license for the first six months after the publication date (see http://www.rupress.org/terms/). After six months it is available under a Creative Commons License (Attribution–Noncommercial–Share Alike 4.0 International license, as described at https://creativecommons.org/licenses/by-nc-sa/4.0/).

PAK2 plays a dual role in apoptosis (Walter et al., 1998; Frank et al., 2012). Full-length PAK2 localizes to cell–cell junctions and inhibits proapoptotic signaling by phosphorylating Bcl-2–associated death promoter (BAD) protein (Jakobi et al., 2001; Marlin et al., 2009). In contrast, a constitutively active C-terminal fragment of PAK2 stimulates apoptosis. Whether PAK2 is pro- or anti-apoptotic is determined via PAK2 cleavage by caspases (Walter et al., 1998). PAK2 is cleaved by caspase-3 at D212, which generates a constitutively active PAK2-p34, a C-terminal fragment that translocates to the nucleus (Jakobi et al., 2003) and stimulates phosphorylation of a new set of substrates, which in turn promote programmed cell death.

Here, we report a novel mechanism regulating cell survival in response to mechanical force. We present evidence that force stimulates PAK2 activation in cell–cell junctions, where it links metabolic signaling by AMPK to an Abl-mediated cell contractility pathway. AMPK binding prevents PAK2 from cleavage and allows cells to survive low amplitudes of force. Upon exposure to higher amplitudes of force, PAK2 is no longer protected by AMPK from cleavage, and a C-terminal PAK2 fragment initiates programmed cell death by translocating to the nucleus—a response that is prevented in cells expressing a cleavage-resistant PAK2 protein. Thus, PAK2 is a force-sensitive protein that protects cells under force from death and plays a key role in linking force-induced mechanotransduction, metabolism, and cell survival.

Results

PAK2 is activated and recruited to the cadherin adhesion complex in response to force

PAK2, a serine/threonine kinase with pro- and anti-apoptotic functions, is activated downstream of E-cadherin (Frank et al., 2012), and phosphorylates myosin light chain (Goeckeler et al., 2000). This close association with E-cadherin and contractility mediators suggests that PAK2 might be sensitive to force. Based on this rationale, as a first measure of the effects of force on PAK2 activation, we treated human epithelial cells (MCF10A) with Calyculin A, a phosphatase inhibitor that increases myosin II phosphorylation and cellular contraction. Treatment with Calyculin A increased PAK2 activation as measured by PAK2 autophosphorylation at a serine required for its activation, i.e., serine 20 (Fig. S1 A) and at threonine 402 in its activation loop (Fig. S1 B). This effect was abrogated when PAK2 expression was inhibited with shRNAs against PAK2 (Fig. S1, A and B).

To determine whether a more physiological force could stimulate PAK2 activation, we applied shear stress (12 dynes/cm^2 for 2 h) to MCF10A cells or human bronchial epithelial cells (Tzima et al., 2005). Shear stress increased PAK2 activation in both cell lines (Fig. 1 A and Fig. S1 C). Importantly, this increase was abrogated in cells expressing two different shRNAs against PAK2 (shPAK2 and shPAK2.2), but not in cells expressing a scrambled shRNA sequence (scPAK2; Fig. 1 A). The increased PAK2 phosphorylation required both force transmission and E-cadherin engagement, as treatment with blebbistatin (a myosin II inhibitor) or HECD-1 (an E-cadherin function–blocking antibody) prevented phosphorylation (Fig. 1 B). Additionally, the effects of shear were specific to PAK2, as shear had no effect on PAK1 activation (Fig. S1 D).

Our observation that the shear stress–induced activation of PAK2 could be blocked by E-cadherin function–blocking antibodies suggests a key role for E-cadherin. To test whether direct application of force on E-cadherin stimulates PAK2, we employed a well-established approach that we and others have used to apply force directly to adhesion receptors (Tzima et al., 2005; Guilluy et al., 2011; Collins et al., 2012; Barry et al., 2014; Bays et al., 2014; Kim et al., 2015). Briefly, magnetic beads coated with E-cadherin extracellular domains were incubated with cells. A permanent ceramic magnet was then used to apply a tensile force to the beads. Previous studies using this approach demonstrated that the results obtained are specific to beads coated with cadherin extracellular domains, as force on beads coated with ligands of other adhesion receptors does not elicit cell contractility (Bays et al., 2014, 2017). Using this approach, application of force increased PAK2 phosphorylation by threefold (Fig. 1 C). The force-dependent activation of PAK2 was inhibited by pretreatment of cells with myosin II inhibitor (blebbistatin; Fig. 1 C) or E-cadherin function–blocking antibodies (HECD-1; Fig. 1 C). Taken together, these data indicate that force on E-cadherin stimulates PAK2 activation.

We examined whether force on E-cadherin induces PAK2 recruitment to the cadherin adhesion complex. To test this possibility, we first examined colocalization of PAK2 and active PAK2 with E-cadherin in cells left resting or subjected to shear stress for 2 h at 12 dynes/cm^2. Shear stress triggered increased PAK2 (Fig. S1 E) and active PAK2 localization (Fig. 1 D) to E-cadherin–containing cell–cell junctions. In contrast, neither active PAK2 nor PAK2 were recruited to focal adhesions in response to force (Fig. 1 E and Fig. S1 F). As a second measure of PAK2 recruitment to E-cadherin, we applied tensile force to magnetic beads coated with cadherin extracellular domains and monitored PAK2 recruitment to the beads. We observed that PAK2 was recruited to the E-cadherin extracellular domain–coated beads in a force- and E-cadherin–dependent manner (Fig. 1 F). Similar binding to E-cadherin was observed in PAK2 immunoprecipitates obtained from cells with tensile force applied directly to the E-cadherin extracellular domain (Fig. 1 G). Taken together, these studies demonstrate that force stimulates PAK2 activation and recruitment to the cadherin adhesion complex.

PAK2 binds directly to AMPK and Abl

We sought to gain insight into whether PAK2 is a component of a known E-cadherin contractility pathway. This signaling cascade is initiated when force triggers E-cadherin to activate AMP-activated protein kinase (AMPK). Active AMPK stimulates an unknown signal transduction cascade culminating in Abelson (Abl)-mediated phosphorylation of vinculin Y822 and the subsequent activation of RhoA-mediated contractility, cell stiffening, and glucose uptake (Bays et al., 2014, 2017). There is evidence consistent with PAK2 mediating the unknown step between AMPK and Abl (Roig et al., 2000; Jung et al., 2008). Based on this rationale, we investigated whether PAK2 was an

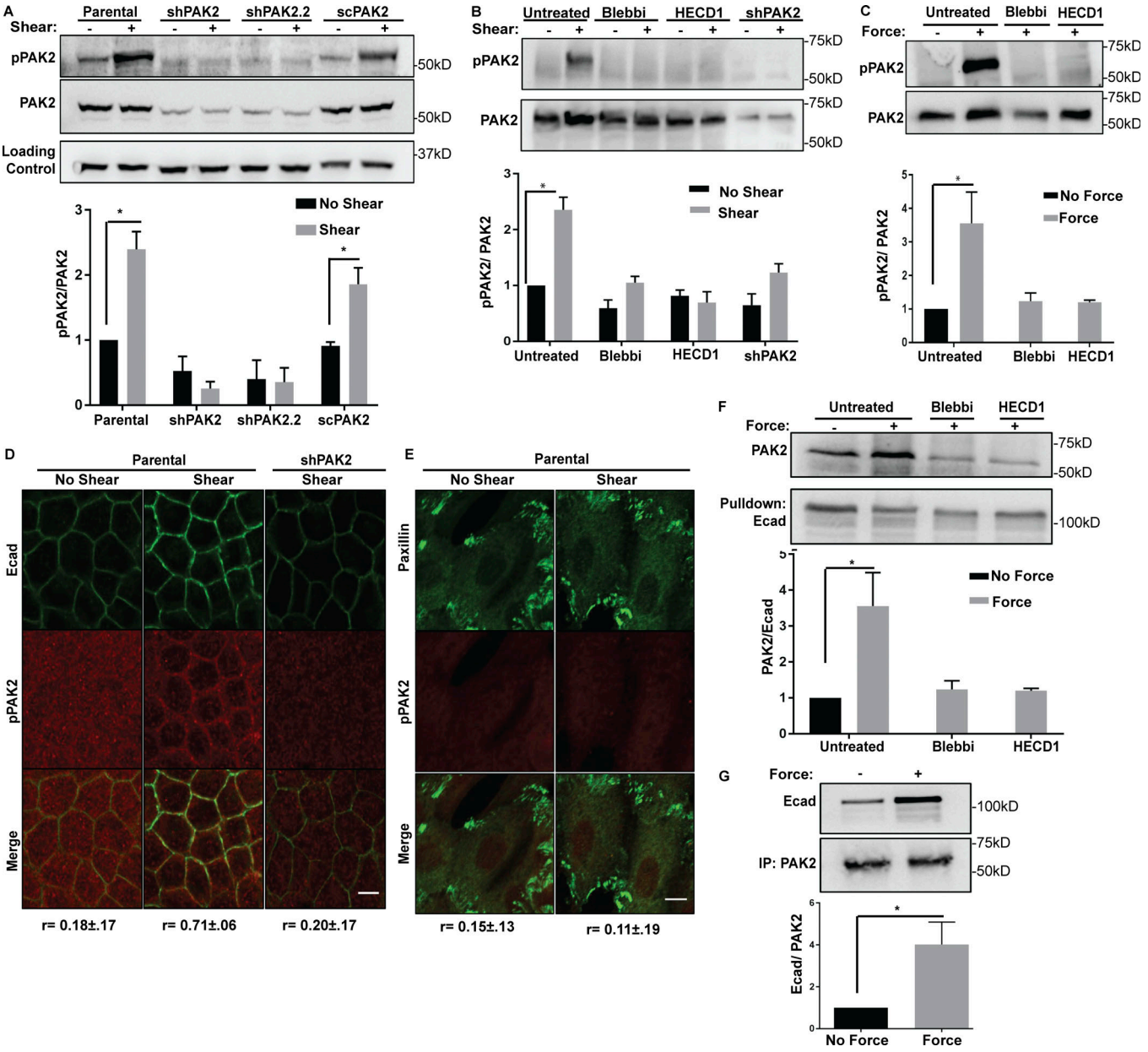

Figure 1. **PAK2 is activated in response to force on E-cadherin and is recruited to the cadherin adhesion complex.** MCF10A cells (parental) or MCF10A cells expressing two different shRNAs against PAK2 (shPAK2 or shPAK2.2) or a scramble shRNA (scPAK2) were employed. **(A and B)** Shear stress increases PAK2 activation. The cells were left resting (–), or shear stress was applied (+). The cells were lysed, and the resulting lysates were immunoblotted with antibodies that recognize phosphorylated PAK2 (pPAK2) or p34 as a loading control and then stripped and reprobed with antibodies that recognize total PAK2 levels; $n = 3$. **(C)** Direct application of force on E-cadherin stimulates PAK2 activation. Magnetic beads coated with cadherin extracellular domains were incubated with the cells, and tensile force was applied using a ceramic magnet. Lysates were blotted as described in A; $n = 3$. **(D and E)** pPAK2 colocalizes with E-cadherin (but not paxillin) in response to force. Shear stress was applied to cells. The cells were fixed, permeabilized, and stained with antibodies against pPAK2 and E-cadherin (Ecad) to visualize cell–cell adhesions (D, $n = 50$), or pPAK2 and paxillin to visualize cell–matrix adhesions (E, $n = 50$). Colocalization of the two proteins was assessed using confocal microscopy; scale bar = 10 µm. An average Pearson correlation coefficient from three independent experiments ± SEM is reported beneath the images. **(F and G)** Force stimulates PAK2 recruitment to E-cadherin. Tensile forces were applied as described in C. The magnetic beads were recovered (F, $n = 3$) or PAK2 was immunoprecipitated (G, $n = 3$), and the coprecipitating levels of PAK2 or E-cadherin were examined by immunoblotting. In A–C, F, and G, representative immunoblots are shown in each panel; the graphs beneath each panel represent the quantification from three independent experiments. *, $P < 0.05$. Blebbistatin (Blebbi) corresponds to cells pretreated with a myosin II inhibitor, and HECD-1 indicates cells pretreated with an E-cadherin function blocking antibody.

intermediate between AMPK and Abl. To probe this interaction, we applied tensile force to parental cells and shPAK2 cells, immunoprecipitated AMPK, and analyzed coprecipitating levels of PAK2 and Abl. In response to force, Abl and PAK2 coprecipitated with AMPK (Fig. 2 A). Importantly, the interaction between AMPK and Abl was lost in cells with depressed levels of PAK2, supporting the notion that PAK2 lies between AMPK and Abl (Fig. 2 A).

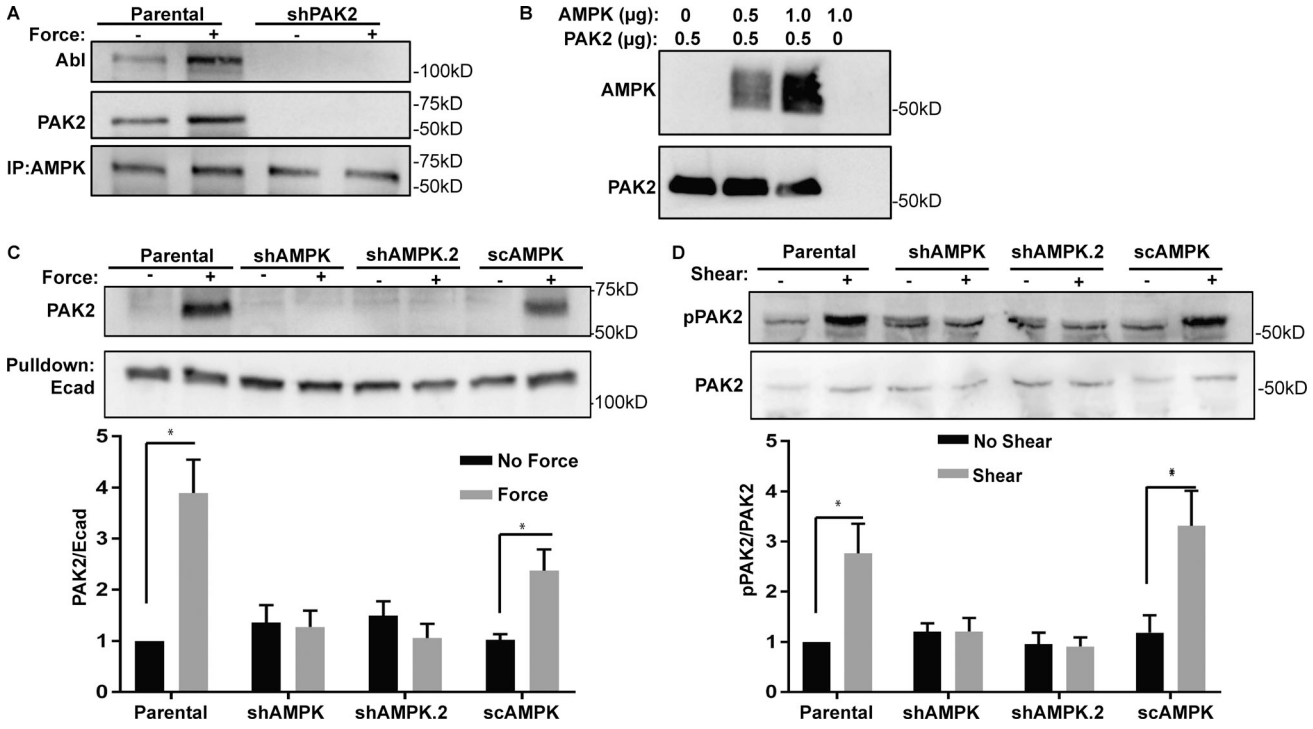

Figure 2. **PAK2 directly binds AMPK, and AMPK is required for PAK2 activation and recruitment. (A)** PAK2 and Abl coimmunoprecipitate with AMPK. MCF10A parental or shPAK2 cells were left resting (–), or tensile forces were applied (+) as described in the legend of Fig. 1 C. AMPK was immunoprecipitated, and the coprecipitating levels of PAK2 or Abl were examined by immunoblotting; $n = 3$. **(B)** PAK2 binds directly to AMPK. Increasing amounts of recombinant His-AMPK were incubated with or without GST-PAK2. The bound protein complexes were isolated and analyzed by immunoblotting; $n = 3$. **(C)** PAK2 recruitment to the cadherin adhesion complex requires AMPK. MCF10A or MCF10A cells expressing different shRNAs against AMPK (shAMPK and shAMPK.2) or a scramble shRNA against AMPK (scAMPK) were left resting (–), or tensile forces were applied (+). Recruitment of PAK2 beneath the E-cadherin–coated beads was assessed by immunoblotting; $n = 3$. **(D)** PAK2 activation requires AMPK. Shear stress was applied (+) to the indicated cell lines, and PAK2 activation was monitored; $n = 3$. Representative immunoblots are shown in each panel, and the graphs beneath the blots represent the quantification of the average amount of protein normalized to a loading control (Ecad) from three independent experiments. *, $P < 0.05$.

To test for direct binding, we first performed an in vitro bind ing assay with recombinant Abl and PAK2. For this, 0 or 1.0 μg of Abl was incubated with 0.5 μg of GST-tagged PAK2 in solution. The GST-PAK2 was recovered, and the coprecipitating levels of Abl were examined by immunoblotting or Coomassie blue staining. We found that recombinant Abl bound to PAK2 (Fig. S2 A) and in an approximately equal ratio (Fig. S2 B). We next examined binding between recombinant PAK2 and AMPK. For this, 0.5 μg of GST-PAK2 was incubated with 0, 0.5, or 1.0 μg of recombinant AMPK in solution, and the complexes were recovered, washed, and detected by immunoblotting with antibodies that recognize PAK2 and AMPK or by staining the gels with Coomassie blue. PAK2 bound directly to AMPK (Fig. 2 B) and in an apparently equal molar ratio (Fig. S2 C). Moreover, we observed a 3.7-fold increase in PAK2 phosphorylation in the presence of AMPK, suggesting that PAK2 is a direct substrate for AMPK (Fig. S2 D).

We next investigated whether AMPK was required for force-induced PAK2 activation and recruitment to the cadherin adhesion complex. We monitored recruitment of PAK2 to magnetic beads coated with E-cadherin extracellular domains in parental cells or two different cell lines in which AMPK expression was suppressed using shRNAs (shAMPK and shAMPK.2). Cells expressing a scramble shRNA (scAMPK) were employed as an additional control. The levels of AMPK in each cell line are shown in Fig. S2 E. PAK2 was robustly recruited to the E-cadherin–coated magnetic beads isolated from the parental cells and the cells expressing the scramble sequence. In contrast, inhibition of AMPK suppressed PAK2 recruitment to the magnetic beads (Fig. 2 C). Similarly, we observed that PAK2 was robustly phosphorylated in the parental and scramble-exp ressing cell lines, and AMPK inhibition abrogated this effect (Fig. 2 D). As a second measure of PAK2 recruitment, we examined colocalization of PAK2 with E-cadherin in cell–cell junctions in cells pretreated with Compound C, a widely employed cell-permeable inhibitor of AMPK. Inhibition of AMPK prevented PAK2 colocalization with E-cadherin in cell–cell contacts (Fig. S1 E). Taken together, these findings suggest that AMPK binds, phosphorylates, and recruits PAK2 to the cadherin adhesion complex, where it binds directly to Abl tyrosine kinase.

PAK2 lies in an E-cadherin mechanosignaling pathway culminating in increased contractility and cell stiffening

Our observation that PAK2 binds directly to Abl suggests it may lie upstream of Abl in an E-cadherin contractility pathway culminating in cell stiffening (Fig. 3 A). To determine whether PAK2 is a component of the contractility pathway, we applied force to parental or shPAK2 cells and monitored downstream Abl activation. As an indicator of Abl activation, we analyzed

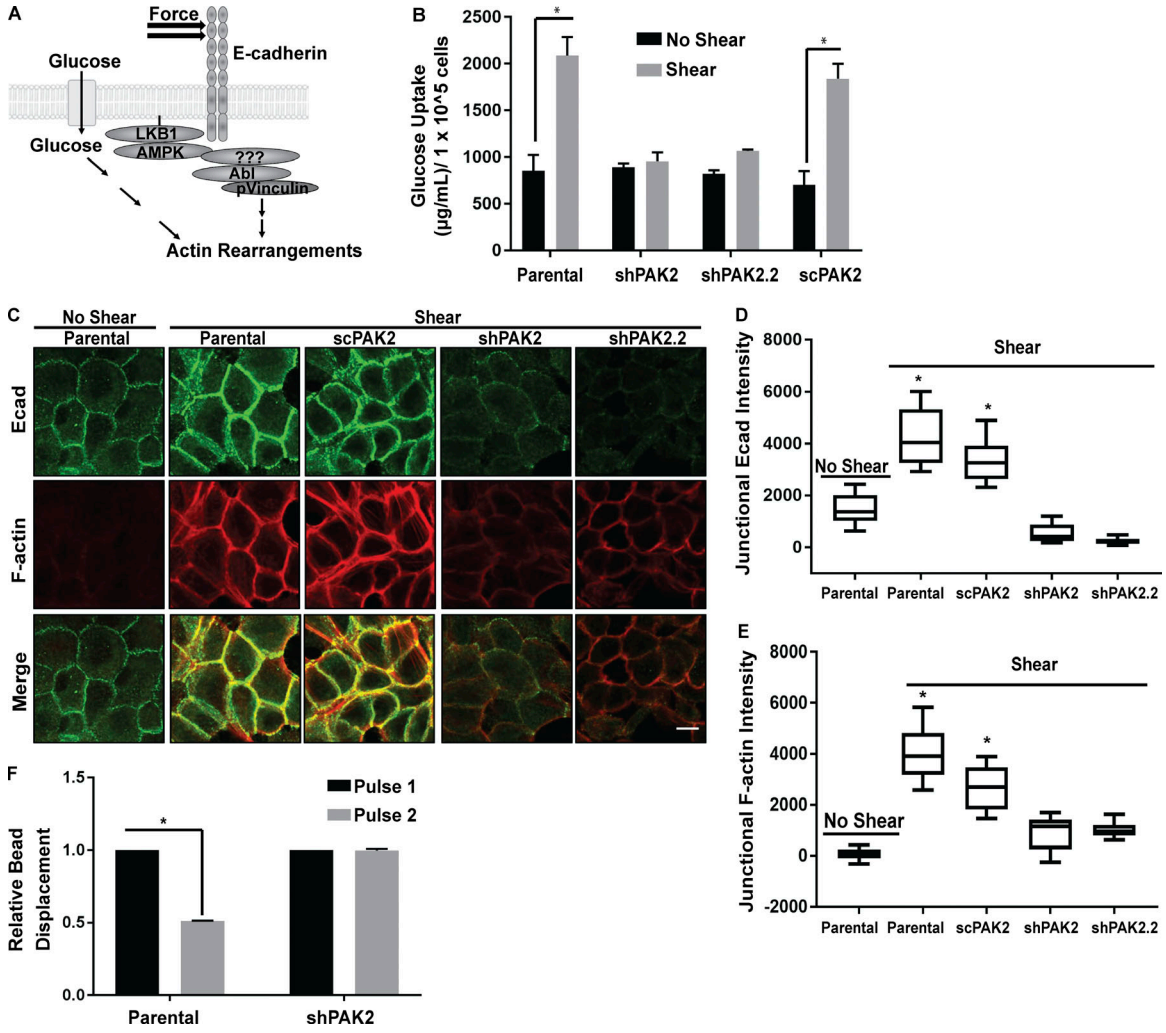

Figure 3. **PAK2 is required for force-induced glucose uptake and increased contractility. (A)** An E-cadherin signaling pathway culminating in elevated contractility. **(B)** Inhibition of PAK2 impairs force induced glucose uptake. The amount of a fluorescently labeled 2-deoxyglucose analogue taken up by the indicated MCF10A cell lines was monitored. The graphs represent average glucose uptake for at least nine representative experiments ± SEM; *n* = 9. **(C–E)** PAK2 is required for reinforcement of cell–cell junctions and the actin cytoskeleton. MCF10A cells (parental) or MCF10A cells expressing two different shRNAs against PAK2 (shPAK2 or shPAK2.2) or a scramble shRNA (scPAK2) were left resting (no shear) or shear stress was applied. The cells were stained with antibodies that recognize E-cadherin (Ecad) or Texas-Red phalloidin and examined by confocal microscopy (C, *n* = 50). The correct fluorescence intensity of E-cadherin (D, E-cad, *n* = 50) or F-actin (E, *n* = 50) in cell–cell junctions are represented by a box-and-whisker plot with median, 10th, 25th, 75th, and 90th percentiles indicated. Scale bars = 10 µM. **(F)** PAK2 is required for adaptive cell stiffening. Pulses of force were applied to E-cadherin–coated magnetic beads that were incubated with parental (*n* = 90) or shPAK2 (*n* = 90) cells. Experiments are the relative means ± SEM normalized to the first pulse. *, P < 0.05 for all panels.

phosphorylation of the Abl substrate, CrkL, at the Abl-specific site. Application of shear stress in parental cells stimulated CrkL phosphorylation, and loss of PAK2 abrogated force-induced CrkL phosphorylation (Fig. S2 F). Thus, the E-cadherin mechanosignaling pathway requires PAK2.

E-cadherin mechanosignaling increases stimulate glucose to be taken up into the cell and oxidized to ATP so that the cell has the energy necessary to support the actin cytoskeletal rearrangements necessary to resist forces applied to the cell (Bays et al., 2017). To determine if PAK2 is required for the uptake of glucose, shear stress was applied to cells, and the uptake of a fluorescently labeled, nonhydrolyzable 2-deoxyglucose was monitored. Force stimulated a 2.5-fold increase in glucose uptake. In contrast, force did not stimulate the uptake of glucose in cells with depressed PAK2 levels (Fig. 3 B). We next examined whether the loss of PAK2 disrupts reinforcement of the actin cytoskeleton. Parental cells, shPAK2, shPAK2.2, and scPAK2 cells were subjected to shear stress, fixed, permeabilized, and stained for E-cadherin and actin. In parental and scPAK2 cells, shear stress induced robust enrichment of E-cadherin and actin at cell–cell junctions (Fig. 3, C–E). In contrast, shPAK2 and shPAK2.2 cells did not display force-induced enrichment of E-cadherin or actin (Fig. 3, C–E). The effects of force were also abrogated by preincubation of the cells with blebbistatin (Fig. 3, C–E). Thus, PAK2 is required for glucose uptake and reinforcement of the actin cytoskeleton.

To determine whether loss of glucose uptake and reinforcement of the actin cytoskeleton directly affects the physiology of the cell, we measured adaptive cell stiffening. For this, we applied tensional forces (using 3D force microscopy to paramagnetic beads coated with antibodies or ligands to endogenous

proteins). Using this approach, pulses of force are applied to the bead, and the cells respond by increasingly resisting bead displacement. In good agreement with published studies, pulses of force applied to parental cells triggered a significant decrease in pulse-to-pulse bead displacement, indicative of force-dependent adaptive stiffening (Bays et al., 2014; Fig. 3 F). In contrast, when force was applied to E-cadherin in the shPAK2 cells, there was a lack of reinforcement in response to pulses of force (Fig. 3 F). Collectively, these data indicate that PAK2 is required for E-cadherin mechanotransduction and cell stiffening.

PAK2 mediates survival in cells under tension

There is some evidence that PAK2 counteracts apoptotic stimuli (Frank et al., 2012). Based on this rationale, we examined the effect that loss of PAK2 has on cell death. Cells were subjected to shear stress, and apoptosis was examined by monitoring the levels of the proapoptotic marker, Bad, and the number of annexin V–positive cells. Application of force to the parental cells did not significantly alter the number of annexin V–positive cells. In contrast, inhibition of PAK2 increased annexin V positivity in a force-dependent manner (Fig. 4 A). Similarly, shear stress had no significant effect on Bad levels in parental cells or scPAK2 cells (Fig. 4 B). In contrast, application of shear stress to the cells lacking PAK2 increased Bad levels (Fig. 4 B). Importantly, this increase in Bad levels was blocked by preincubation of the cells with the E-cadherin function blocking antibody, HECD1 (Fig. 4 C), indicating an essential role for this adhesion receptor. In further support of a role for E-cadherin, direct application of force to this adhesion receptor in parental cells using the magnetic bead approach did not change apoptosis (Fig. 4 D). In contrast, the force-stimulated Bad levels were increased in the shPAK2 cells (Fig. 4 D). Finally, to ensure that the increased apoptosis was specific to loss of PAK2 and not related to the overall health of the cells, we sickened cells by treatment with increasing doses of etoposide, a DNA-damaging agent, and investigated whether force increased apoptosis. At all doses examined, the levels of Bad did not increase when the cells were pretreated with etoposide (Fig. 4 E). Hence, PAK2 protects cells exposed to force from death.

All the studies we performed thus far were done using 12 dynes/cm^2 of force, which is the amount of force that endothelial cells experience from the flow of blood or in response to airflow (Ridge et al., 2005; Tzima et al., 2005; Flitney et al., 2009). In the body, cells do not die upon experiencing this amplitude of force; rather apoptosis occurs only when higher levels of force are applied (Yoon et al., 2001; Bilek et al., 2003; Ridge et al., 2005; Mahto et al., 2014). To determine if we could mimic the effect of force on apoptosis, MCF10A cells were exposed to increasing levels of orbital shear stress, ranging from no force (0 rpm = 0 dynes/cm^2) to high levels of physiological force (400 rpm = 27 dynes/cm^2). Exposure of MCF10A cells to this amount of force and larger has been routinely employed in previous studies (Byers et al., 1995; Tözeren et al., 1995; Paszek et al., 2005; Mitchell et al., 2015; Fuhrmann et al., 2017). Importantly, the maximum force amplitudes we employ in this study are a magnitude lower than the amount of force epithelial cells experience during coughing or peristalsis (Ridge et al., 2005; Flitney et al., 2009; Button and Button, 2013).

In the absence of force or in the presence of low levels of force, Bad levels were consistently low in MCF10A cells, indicating little to no cell death. As the level of force increased past 12 dynes/cm^2 (200 rpm), Bad levels increased (Fig. 5 A). This observation is in good agreement with numerous previous studies indicating that high levels of physiological force trigger apoptosis (Bilek et al., 2003; Ridge et al., 2005; Mahto et al., 2014). Because the data in Fig. 4 indicated that PAK2 protects against apoptosis, we examined PAK2 activation in response to orbital shear stress ranging from 0 to 27 dynes/cm^2. In the absence of force, PAK2 activation was low and gradually increased until it reached a peak at physiological levels (200 rpm or 12 dynes/cm^2; Fig. 5 B). After physiological levels of force were reached, PAK2 activation began to diminish until it reached basal levels at 300 rpm or 19 dynes/cm^2. These observations indicate that when PAK2 is active, apoptosis is low, and when PAK2 is inactive, apoptosis increases.

Cleaved PAK2 stimulates apoptosis, and AMPK protects against cleavage

We consistently noticed a decrease in total PAK2 levels as the amount of force applied was elevated past 12 dynes/cm^2 (Fig. 5 B). It is well established that PAK2 is cleaved in response to death stimuli and translocates to the nucleus, where it stimulates transcription of apoptotic genes (Walter et al., 1998). Based on this rationale, we investigated the effects of force on PAK2 cleavage using an antibody that recognizes the truncated product. Little to no cleaved PAK2 was observed in cells under physiological levels of force (Fig. 5 C). However, as the amplitude of the force was increased past 300 rpm (19 dynes/cm^2), PAK2 cleavage dramatically elevated (Fig. 5 C). Consistent with previous studies, the level of cleavage was directly related to the extent of apoptosis (Fig. 5, A and C; Walter et al., 1998).

Cleavage-resistant forms of PAK2 survive all amplitudes of force

Our results indicate a key role for PAK2 cleavage in mediating the apoptotic response of cells experiencing high forces. To test whether PAK2 cleavage is essential for force-induced apoptosis, we generated a cleavage-resistant D212E PAK2 and expressed it in MCF10A cells with depressed levels of PAK2. As a control, we rescued the PAK2 knockdown cells with human PAK2 (WT). Immunoblotting of cell lysates revealed that the mutant PAK2 was expressed (Fig. 6 A), activated (Fig. 6 B), and stimulated downstream signaling (Fig. 6 C) to WT levels. In contrast with cells expressing WT PAK2, no PAK2 proteolysis was observed in cells expressing the D212E cleavage-resistant protein even when high amplitudes of force were applied (Fig. 6 D). To test whether the cleavage-resistant mutant protected cells from death, increasing levels of shear stress were applied to cells and Bad levels were monitored via immunoblotting or the percentage of annexin V–positive cells was determined. When physiological (Fig. 6 E) and elevated (Fig. 6 F) levels of force were applied, cells expressing cleavage-resistant PAK2 did not have elevated levels of Bad or annexin V positivity (Fig. 6, E–G). Collectively, these data indicate that preventing PAK2 cleavage protects cells against death.

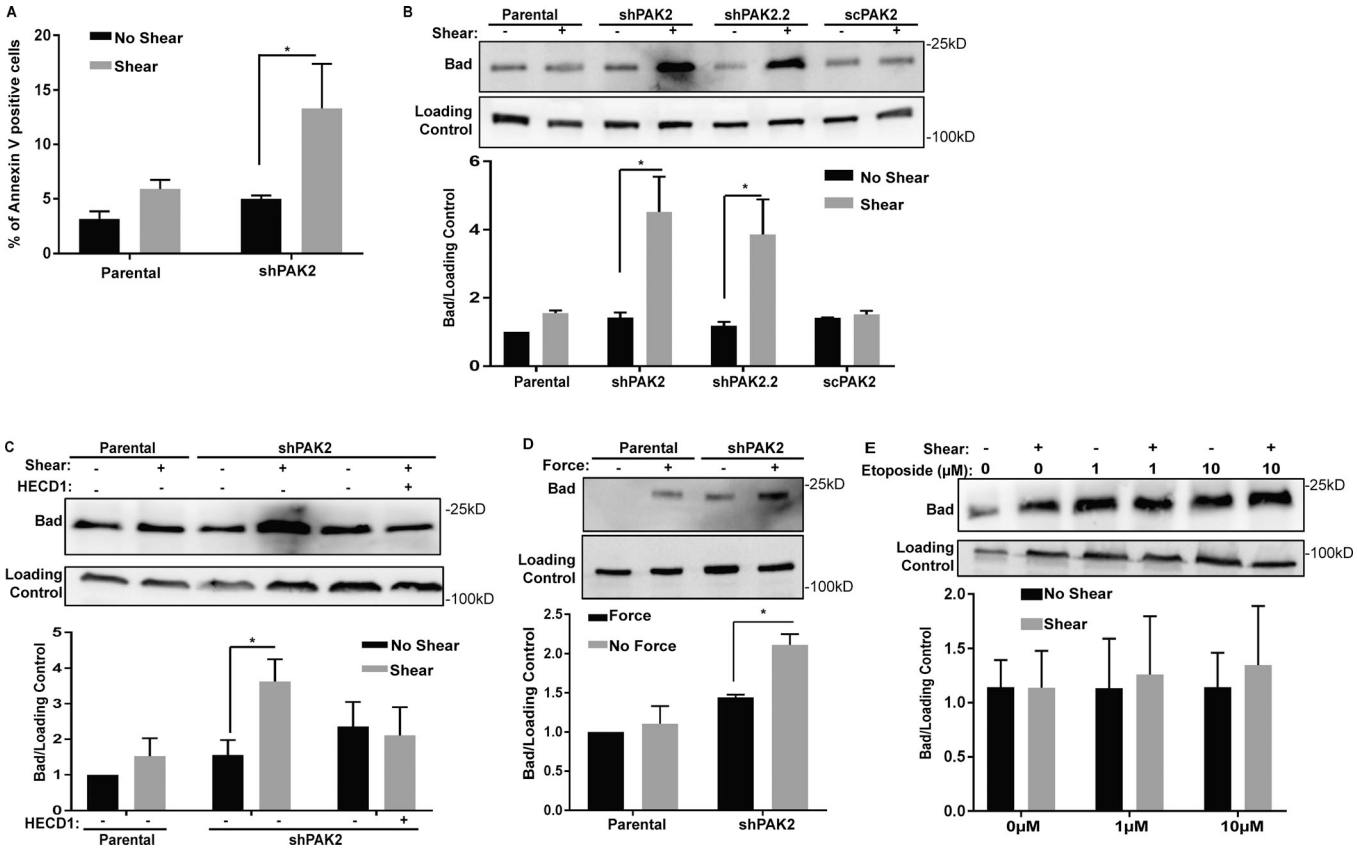

Figure 4. **PAK2 protects cells under force against cell death.** Shear stress (A–C and E) or tensile forces (D) were applied to MCF10A cells (parental) or MCF10A cells expressing two different shRNAs against PAK2 (shPAK2 and shPAK2.2) or MCF10A cells expressing a scramble shRNA against PAK2 (scPAK2). **(A–D)** PAK2 protects against apoptosis. In A, cells were lifted off dishes, washed with PBS, and stained with APC-annexin V, and the number of positive cells was scored using flow cytometry. The percentage of annexin V–positive cells in the presence or absence of shear is shown; *n* = 3. In B–D, whole-cell lysates were immunoblotted with antibodies against the proapoptotic marker, Bad, and a loading control; *n* = 3 (Ecad). **(E)** The cells were treated with increasing concentrations of etoposide to sicken the cells before application of force with the goal of demonstrating that cells under force were not dying because they are sicker; *n* = 3. The graphs beneath the immunoblots in B–E show the average ± SEM for three independent experiments. *, P < 0.05.

AMPK protects PAK2 against cleavage and the subsequent force-induced apoptosis

Our data in Fig. 2 indicate that AMPK recruits PAK2, and previous work suggests that binding partners may protect PAK2 from cleavage (Luo and Rubinsztein, 2009). Based on this rationale, we first tested if AMPK protects cells under force from cleavage. For these studies, we treated parental, shAMPK, shAMPK.2, and scAMPK cells with physiological levels of force and monitored PAK2 cleavage. No change in PAK2 was noted in parental or scAMPK cells exposed to physiological levels of shear stress (Fig. 7 A). In contrast, cells lacking AMPK show modest, but statistically insignificant, elevations in PAK2 cleavage in the absence of force and robust increases in PAK2 cleavage upon exposure to force, suggesting that AMPK may protect PAK2 from cleavage (Fig. 7 A). Cleaved PAK2 is known to translocate to the nucleus and promote transcription of proapoptotic genes. Therefore, we subjected parental, shAMPK cells, and scAMPK cells to shear stress and monitored cleaved PAK2 colocalization with the nucleus. In response to shear stress, cleaved PAK2 localizes in and around the nucleus in shAMPK cells only as visualized by staining with DAPI and an antibody that recognizes cleaved PAK2 (Fig. 7 B). To directly test whether AMPK can protect PAK2, we incubated recombinant PAK2 with caspase 3 (the PAK2 cleavage enzyme) in the presence or absence of recombinant AMPK. In the absence of AMPK, PAK2 was readily cleaved by caspase 3 (Fig. 7 C and Fig. S2 H). In contrast, preincubation with AMPK prevented PAK2 proteolysis (Fig. 7 C and Fig. S2 H). This effect was specific for AMPK, as addition of another protein, BSA, did not prevent caspase cleavage (Fig. 7 C and Fig. S2 I). Also of note, AMPK phosphorylation was high in cells under physiological levels of force and decreased as the amplitude of the force increased, suggesting that PAK2 protection from cleavage requires AMPK activation (Fig. S2 G). Collectively, these data indicate that cells experiencing physiological levels of force do not undergo cell death, because AMPK ensures PAK2 integrity and activation. In contrast, cells experiencing higher amplitudes of force apoptose, because PAK2 is unprotected, cleaved, and inactivated.

These observations suggest that AMPK regulates force-induced apoptosis by virtue of its ability to activate and protect PAK2 against proteolysis. To test this possibility directly, we determined if constitutively active or cleavage-resistant PAK2 could overcome the requirement for AMPK in cells. For this, we overexpressed WT, constitutively active (T402E), or cleavage-resistant (D212E) PAK2 in MCF10A cells and cells lacking AMPK (shAMPK) to a

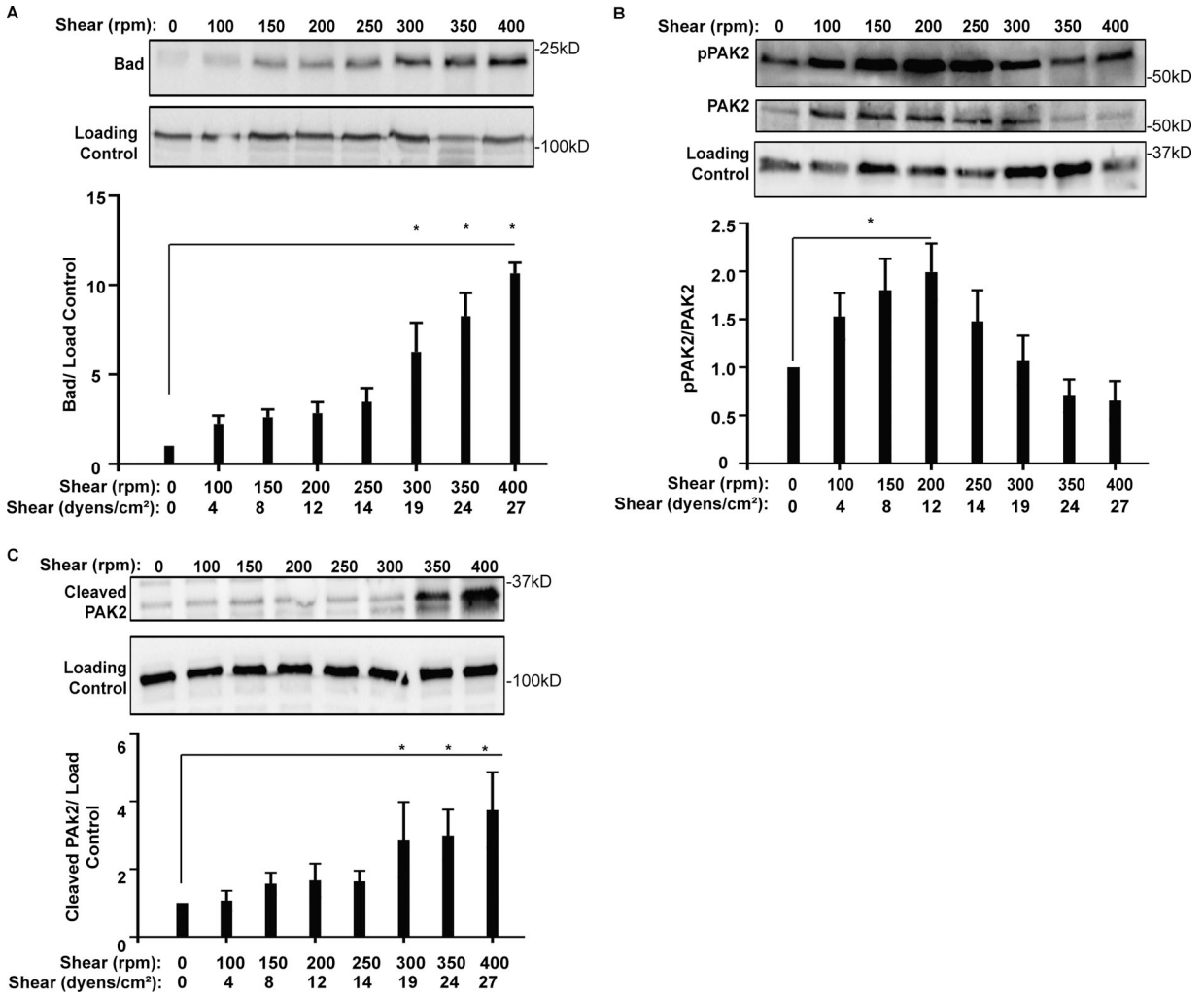

Figure 5. **High levels of physiological force induce apoptosis by stimulating PAK2 inactivation and cleavage. (A–C)** Forces stimulate apoptosis, PAK2 inactivation, and cleavage. MCF10A cells were subjected to different amplitudes of orbital shear stress ranging from 0 to 400 rpm (27 dynes/cm²). In A, high physiological forces stimulate apoptosis. The cells were lysed, and lysates were immunoblotted with antibodies against Bad or a loading control; *n* = 3. In B, high physiological forces trigger PAK2 inactivation. The lysates were immunoblotted with antibodies against phospho-PAK2, PAK2, or a loading control; *n* = 3. In C, high physiological forces promote PAK2 cleavage. Lysates were immunoblotted with antibodies against cleaved PAK2 or a loading control; *n* = 3. The graphs beneath the images show the average ± SEM for three independent experiments. *, P < 0.05.

similar extent (Fig. 7 D) and examined the effect of force on apoptosis. When low levels of force were applied to cells lacking AMPK and expressing WT PAK2, Bad levels were elevated (Fig. 7 E). In contrast, application of force to cells expressing the cleavage-resistant or constitutively active PAK2 did not undergo apoptosis in response to force (Fig. 7 E). Thus, the requirement for AMPK can be overcome by expression of PAK2 proteins that are constitutively active or cleavage resistant. Taken together, these data indicate that PAK2 is a mechanoprotective factor whose function is controlled by AMPK.

Discussion

Many studies have focused on how cells respond to force, with little attention paid to how this event is integrated with other cellular processes, such as cell survival. At the outset of this work, we were motivated to identify factors that protect cells under force from death. Here, we demonstrate that a consequence of force on E-cadherin is recruitment and activation of PAK2. PAK2 lies upstream of E-cadherin contractility and cell stiffening and is an important determinant of cellular apoptosis. Together, these observations led us to suggest that this interaction is one way that E-cadherin mechanotransduction is linked to cell survival. Further evidence supporting this idea comes from our studies of mutant PAK2s. Whereas AMPK binds and protects PAK2 from proteolysis to ensure cell survival under low forces, higher amplitudes of force stimulate the cleavage of PAK2 and increased phosphorylation of substrates, leading to programmed cell death. This concept is further supported by our findings that cleavage-resistant forms of PAK2 survive even the highest of forces applied to cells. Taken together, these data indicate that epithelial cells under strain are protected from death by PAK2. One advantage of a protection mechanism may be to allow the epithelium to adapt to fluctuations in mechanical

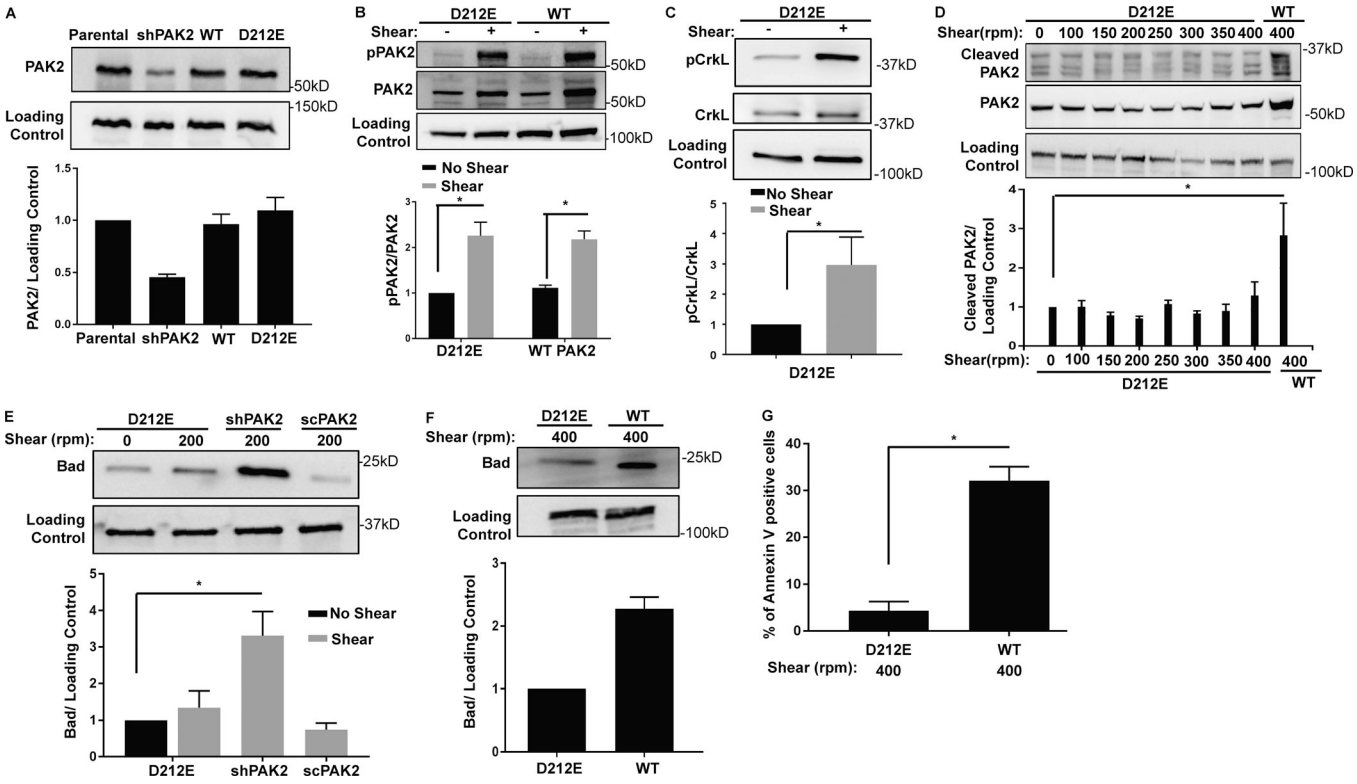

Figure 6. **Cleavage-resistant PAK2 protects against force-induced apoptosis.** MCF10A cells (parental), MCF10A cells expressing a shRNA against PAK2 (shPAK2), or MCF10A shPAK2 cells reexpressing a cleavage resistant D212E mutant or a WT version of PAK2 were left resting (–), subjected to physiological levels of shear stress (+), or subjected to the indicated amplitudes of shear stress. **(A)** The cleavage-resistant mutant PAK2 and WT PAK2 are expressed at endogenous levels in the shPAK2 cells. The levels of PAK2 in cell lysates were examined by immunoblotting; *n* = 3. **(B and C)** PAK2 activation and downstream signaling are unaffected by the D212E mutation. Lysates were immunoblotted with antibodies that recognize: phosphorylated PAK2 as an indicator of activation (B, *n* = 3) or phosphorylated CrkL (pCrkL) at the Abl-specific sites as an indicator of downstream Abl signaling (C, *n* = 3). The immunoblots were then stripped and reprobed with antibodies that recognize the total protein levels or a loading control. **(D)** A cleavage-resistant mutant PAK2 was not cleaved even at high amplitudes of force. Cells were subjected to the indicated amplitudes of shear stress, and the levels of cleaved PAK2, total PAK2, or a loading control were examined by immunoblotting; *n* = 3. **(E–G)** The cleavage-resistant mutant PAK2 protects against apoptosis at physiological (E, *n* = 3) and high physiological (F and G) forces; *n* = 3. Cells were subjected to the indicated amplitudes of shear stress, and the levels of the proapoptotic marker Bad were examined by immunoblotting. In G, shear stress was applied. The cells were lifted, washed with PBS, and stained with APC-annexin V. The number of positive cells was scored using flow cytometry; *n* = 3. In all panels, the graphs beneath the image show the average ± SEM for three independent experiments. *, P < 0.05.

load and the metabolic demands of responding to it, while maintaining homeostasis and preventing the loss of structure and function.

This work is innovative because it provides a mechanism for how cells under force are protected from cell death. That mechanism involves AMPK-mediated activation and protection of PAK2 at low levels of force; and at higher levels of force, a PAK2 susceptibility to proteolysis and the initiation of a proapoptotic cascade. In the course of identifying a mechanism, we also made the advanced observation that mechanosignaling is controlled by the amplitude of force applied to cells. Many studies report mechanosignaling pathways with little attention to the amplitude of force or the transient nature of the signaling response. The new information in this study calls for more attention to complexities of mechanosignaling response.

We considered the possibility that some of our effects could be the result of an effect of PAK2 on cell–matrix adhesions. Many early studies indicate a role for group I PAK family members, including PAK1, PAK2, and PAK3, in modulating cytoskeletal reorganization, membrane protrusion, cell adhesion, and focal adhesion dynamics. Because the vast majority of these early studies employed pan antibodies that recognize at least PAK1–3, the contribution of each PAK family member to these events emerged later. From this work, we now know that PAK1 and PAK2 do not have overlapping functions. Additionally, PAK1 plays a critical role in cell–matrix adhesions. In fibroblasts, Pak1 is localized to the leading edge of migrating cells and regulates lamellipodial protrusion (Sells et al., 1999, 2000) and the assembly and disassembly of focal adhesions (Manser et al., 1997; Nayal et al., 2006). In contrast, the role of PAK2 in cell–matrix adhesion is less well understood, with its localization to cell–matrix adhesions occurring primarily in cancer cell lines or migratory cells with large lamellipodial protrusions (Coniglio et al., 2008; Delorme-Walker et al., 2011). To determine if the effects we observed in our studies could be an indirect result of an effect of PAK2 on cell–matrix events, we tested whether active PAK2 localizes to focal adhesions and/or focal adhesion dynamics. Active PAK2 localized to cell–cell contacts but did not localize to cell–matrix adhesions (Fig. 1, D and E). Moreover, inhibiting PAK2 had no effect on focal adhesion size or number

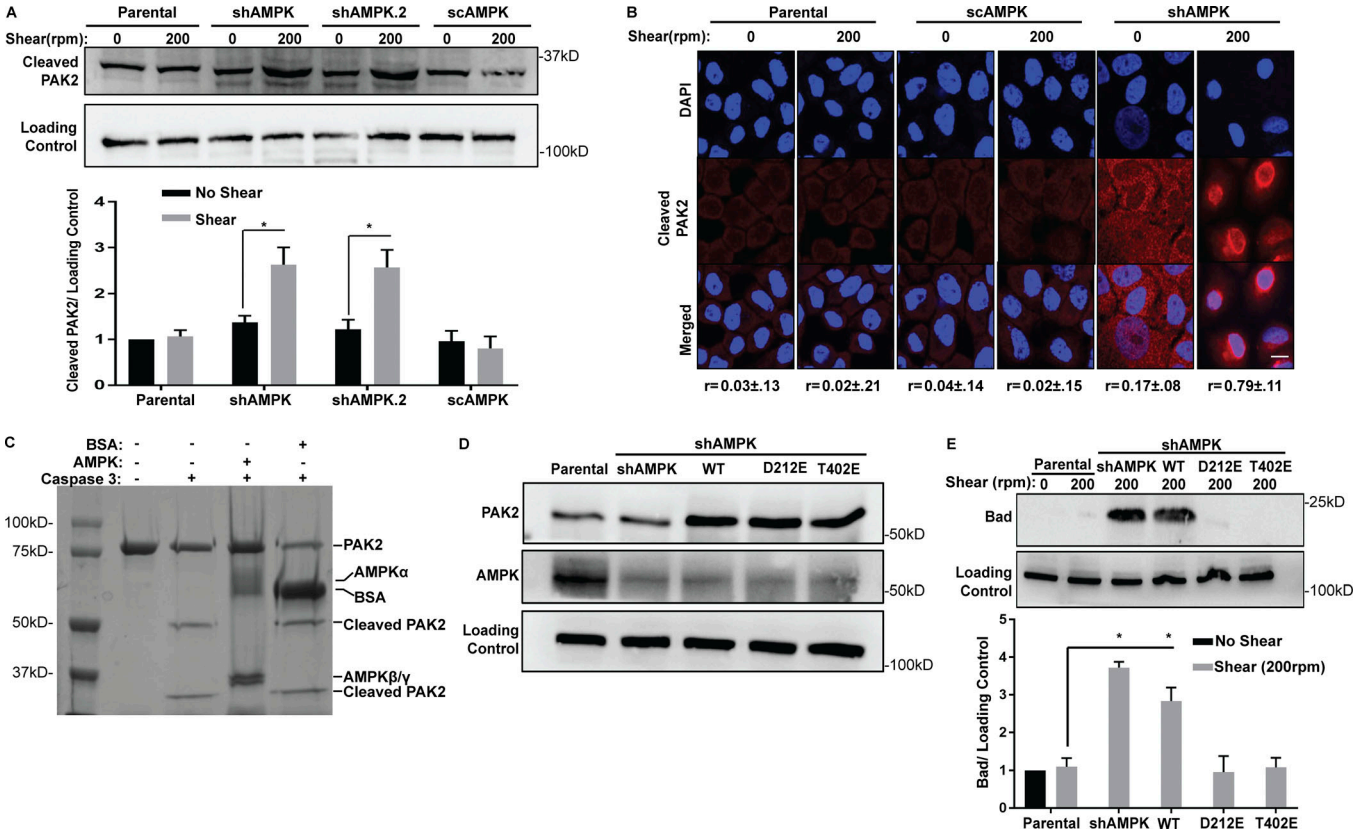

Figure 7. **AMPK protects PAK2 against cleavage. (A)** AMPK protects PAK2 against cleavage in cells. MCF10A cells, MCF10A cells expressing shRNAs against AMPK (shAMPK, shAMPK.2), or MCF10A cells expressing a scramble shRNA against AMPK (scAMPK) were subjected to physiological levels of shear stress, i.e., 12 dyens/cm^2. The levels of cleaved PAK2 were examined by immunoblotting with an antibody that recognizes cleaved PAK2; n = 3. **(B)** Cleaved PAK2 localizes in and around the nucleus in cells lacking AMPK. Parental, shAMPK cells, and scAMPK cells were left resting (no shear) or subjected to shear, fixed, permeabilized, and stained with an antibody that recognizes cleaved PAK2 and DAPI; n = 50. An average Pearson correlation coefficient from three independent experiments ± SEM is reported beneath the images. **(C)** AMPK specifically protects PAK2 from cleavage in vitro. Recombinant PAK2 was incubated with recombinant caspase 3 in the absence (–) or presence (+) of recombinant AMPK or in the absence (–) or presence (+) of BSA. The resulting products were separated on a gel and visualized using Coomassie staining; n = 3. **(D and E)** Constitutively active and cleavage resistant forms of PAK2 bypass the requirement for AMPK protection in cells. WT PAK2, cleavage resistant (D212E) PAK2, or constitutively active (T402E) PAK2 were overexpressed in MCF10A cells with depressed levels of AMPK (shAMPK). In D, lysates were immunoblotted with antibodies against PAK2 and AMPK to reveal the level of each expressed protein and a loading control (p34); n = 3. In E, the cells were left resting or subjected to shear stress (200 rpm), and lysates were immunoblotted with antibodies against Bad or a loading control; n = 3. The graphs beneath the image show the average ± SEM for three independent experiments. *, P < 0.05.

(Fig. S1 F). Thus, our data are consistent with a role of PAK2 that is independent of cell–matrix adhesion. In further support of this notion, we (Bays et al., 2017) and others (Bertocchi et al., 2017) have found that other signaling components of the E-cadherin contractility pathway are stimulated independently of cell–matrix adhesive events.

We were curious whether cells lacking PAK2 would uptake glucose when force was applied. Previously, we reported that application of force to E-cadherin stimulates the uptake of glucose and its metabolism to ATP. The resulting increases in ATP were required to support the actin cytoskeletal rearrangements necessary for the cell to resist force. We further observed that force-stimulated glucose uptake required AMPK activation (Bays et al., 2017). It has remained unclear whether AMPK directly stimulates the uptake of glucose or signals for downstream cytoskeletal rearrangements that require glucose. In the PAK2 knockdown cells employed in this study, AMPK activation is intact, but the force-induced cytoskeletal rearrangements are perturbed (Fig. 3 C), thereby providing us with a cell system to distinguish whether force-induced glucose uptake is stimulated directly by AMPK or indirectly via the increased metabolic demand necessary to support the actin cytoskeleton. To distinguish between these possibilities, we monitored force-stimulated glucose uptake in the PAK2 knockdown cells. Our data in Fig. 3 B indicate that shPAK2 cells lines do not take up glucose in response to application of shear stress. Thus, force stimulates AMPK, which triggers downstream cytoskeletal rearrangements, which signal for more glucose uptake. More work is needed to determine how the cytoskeletal rearrangements signal for increased glucose uptake.

It is notable that AMPK binding protects PAK2 from cleavage (Fig. 7 C). In other systems, death stimuli increase PAK2 proteolysis into a cleavage fragment that translocates to the nucleus and increases the transcription of proapoptotic genes. Our data demonstrate for the first time that AMPK binds directly to PAK2 (Fig. 2 B). Additional in vitro data, which was confirmed in cell lines, indicates that this binding event protects PAK2 from

cleavage by caspases (Fig. 7, A and B). Thus, AMPK is a novel PAK2 binding partner, and this interaction prevents PAK2 from proteolysis. Only one other protein is known to have a similar function. Huntington, the protein that causes Huntington's disease when mutated to include a polyglutamine expansion, protects cells from Fas-induced apoptosis by binding to PAK2 and preventing its cleavage (Luo and Rubinsztein, 2009). Thus, protein binding is emerging as a mechanism to protect PAK2 from destruction. This new information calls for a reevaluation of other binding partners and their potential to protect PAK2 against cleavage.

This newly described role for AMPK in protecting PAK2 from caspase-mediated cleavage suggests that AMPK has multiple roles in a cell under force. Previously, we reported that AMPK is recruited and activated to the E-cadherin adhesion complex in response to force (Bays et al., 2017). One consequence of recruitment was an increase in glucose uptake and the metabolism of glucose to ATP. The resulting ATP provided the energy necessary to reinforce the actin cytoskeleton and prevent force-induced cellular deformation (Bays et al., 2017). Here we show that an additional role for AMPK is to recruit, activate, and protect PAK2 (Fig. 2, A–E; and Fig. 7, A and B). The consequence of PAK2 is a protection against forced-induce cell death (Fig. 6, E and F). Collectively, these findings suggest the existence of a single, highly integrated mechanosignaling pathway downstream of E-cadherin that allows the cell to withstand force by elevating contractility, heightening metabolism, and ensuring survival. A key component of this pathway is AMPK, which not only stimulates metabolism but also controls cell survival. The existence of such a pathway suggests that the cell, like the organism itself, is capable of responding to environmental conditions to adjust its metabolism and ensure its survival. This new information can serve as a platform for understanding how diseases with mechanical, metabolic, and survival disturbances develop and progress.

Materials and methods

cDNAs and viral particles

shRNA lentiviral particles targeting PAK2 and AMPK were purchased from Santa Cruz (36183-V denoted shPAK2.2 and 29673-V denoted shAMPK; Bays et al., 2017). Endogenous PAK2 was silenced using pSUPER-shPAK2, a cDNA that was generated by annealing and subcloning oligonucleotides targeting the human 3′ UTR of PAK2 into the retroviral vector, pSUPER-RETRO PURO (Oligoengine). The sequences used were 5′-GATCCCCCTGCATAACCTGAATGAAATTCAAGAGATTTCATTCAGGTTATGCAGTTTTTA-3′ and 5′-AGCTTAAAAACTGCATAACCTGAATGAAATCTCTTGAATTTCATTCAGGTTATGCAGGGG-3′. Cells expressing pSUPER-shPAK2 are denoted shPAK2 cells. As a control, a scramble oligonucleotide of the PAK2 sequence was also used: 5′-GATCCCCCTGCATAACCTGAATGAAATTCAAGAGATTTCATTCAGGTTATGCAGTTTTTA-3′ and 5′-AGCTTAAAAAACTGCATAACCTGAATGAAATCTCTTGAATTTCATTCAGGTTATGCAGGGG-3′ (denoted scPAK2). The PAK2 mutant (D212E) and (T402E) mutant was synthesized and cloned into the Clontech retroviral vector pLCNX^2 by GenScript.

Cell lines

MCF10A human breast epithelial cells and primary human bronchial epithelial cells were acquired from ATCC and Lonza. MCF10A cells were cultured in DMEM/F12 (1:1) medium with 5% horse serum, 10 µg/ml insulin, 500 U of penicillin/streptomycin, 100 ng/ml cholera toxin, 20 ng/ml EGF, and 0.5 mg/ml hydrocortisone. Cell lines were used for ≤10 passages. In addition, the virus-producing cell line 293GPG, a derivative of 293T cells, was used and maintained as described previously (Maiers et al., 2013; Bays et al., 2014). Briefly, 293GPG cells were grown in DMEM including 10% heat-inactivated FBS, 20 mM Hepes, 0.5 mg/ml G418, 1 µg/ml tetracycline, 2 µg/ml puromycin, 2 mM L-glutamine, and 500 U of penicillin/streptomycin. For retrovirus production, 293GPG cells were cultured in virus-producing medium including DMEM with 10% heat-inactivated FBS, 20 mM Hepes, 500 U penicillin/streptomycin, and 2 mM L-glutamine. To generate shPAK2 cells or scPAK2, the virus-producing cell line 293GPG was transfected with the pSUPER-shPAK2 or pSUPER-scPAK2 construct, respectively. Virus was collected for 5 d and concentrated using high-speed centrifugation. MCF10A human breast epithelial cells were infected with the concentrated virus and selected with puromycin. To generate shPAK2.2 cells, MCF10A cells were infected with the purchased lentiviral particles targeting PAK2, and the cells were selected with puromycin. To generate shPAK2 cells reexpressing WT PAK2 or D212E PAK2, 293GPG cells were transfected with the pLCNX^2-WT PAK2 or pLCNX^2-D212E PAK2 construct. Virus was collected and concentrated as previously described. shPAK2 cells were infected with the concentrated virus and selected with G418. shAMPK, shAMPK.2, and scAMPK cells were generated using commercially available lentiviral particles. MCF10A cells were infected with the lentiviral particles targeting AMPK or lentiviral particles containing a scramble shRNA against AMPK. The cells were then selected with puromycin. To generate the shAMPK cells expressing WT-PAK2, D212E-PAK2, and T402E-PAK2, 293GPG cells were transfected with the pLCNX^2-WT PAK2, pLCNX^2-D212E PAK2, or pLCNX^2-T402E PAK2 construct, and virus was collected and concentrated. Following virus concentration, shAMPK cells were infected and selected with G418.

Magnetic bead force assays

1.5 mg of Dynabeads Protein A (Invitrogen) were incubated with 10 µg of Fc-E-cadherin (Acro Biosystems). The beads were allowed to adhere to confluent cells at 37°C for 40 min. Tensional force was applied for 10 min using a permanent ceramic magnet placed at a distance of 0.6 cm from the cell surface. Following application of force, the cells were immediately lysed using 2× Laemmli sample buffer. As controls, cells were pretreated with blebbistatin (50 µM; Sigma) or HECD-1 (200 µg/ml; Invitrogen) for 2 h.

Orbital shear stress

Tissue culture dishes containing medium were placed on an orbital shaker and rotated at the indicated rpm for 37°C for 2 h. The cells were placed on ice, washed in ice-cold PBS, and lysed in 2× sample buffer.

Calyculin A treatment

Confluent cells were treated with 5 nM of Calyculin A (Cell Signaling) for 40 min, transferred to ice, and immediately lysed using 2× Laemmli sample buffer.

Immunoprecipitation

To immunoprecipitate PAK2 or AMPK, cells were lysed in EB buffer (1 mM Tris-HCl, pH 7.6, 50 mM NaCl, 1% Triton X-100, 5 mM EDTA, 50 mM NaF, 20 µg/ml aprotinin, 2 mM Na_3VO_4, and 1 mM PMSF). A 1:100 dilution of an antibody against PAK2 (2608; Cell Signaling) or AMPK (2532; Cell Signaling) was incubated with lysates for 1.5 h. The complexes were recovered using Protein A agarose beads (Sigma), washed extensively, resuspended in Laemmli sample buffer, and analyzed by immunoblotting.

Pulldown assays

Following application of tensional forces as described above, the cells were lysed in lysis buffer (20 mM Tris, pH 7.6, 150 mM NaCl, 0.1% NP-40, 2 mM $MgCl_2$, and 20 µg/ml aprotinin). Fc-cadherin–coated beads were recovered from the cell lysates using a permanent ceramic magnetic, washed in lysis buffer, and then resuspended in Laemmli sample buffer.

Immunoblotting

Samples were fractioned by SDS-PAGE and transferred to PVDF (Immobilon). The resulting membranes were blocked in 5% milk (E-cadherin, vinculin, and p34) or 5% BSA (PAK1, pPAK1, PAK2, pPAK2, AMPK, BAD, Abl, pCrkl, Crkl, and cleaved PAK2). PAK1, pPAK1, PAK2, and pPAK2 were recognized with rabbit polyclonal antibodies from Cell Signaling (2602, 2605, 2608, and 2607, respectively). Abl kinase was recognized using a rabbit polyclonal antibody from Santa Cruz (clone K-12). E-cadherin was recognized using a mouse monoclonal antibody from BD Biosciences. Vinculin was detected using a mouse monoclonal vinculin antibody (hVin1; Sigma). Bad was recognized using a rabbit monoclonal antibody from Cell Signaling (9239). AMPK was detected using a rabbit polyclonal antibody from Cell Signaling (2532). pCrkl was recognized using a rabbit antibody from Cell Signaling (3181), while Crkl was recognized via a mouse antibody from Santa Cruz (C-20). Cleaved PAK2 was detected using a mouse monoclonal antibody that recognizes the C terminus of PAK2 at an epitope located between residues 497 and 522 (sc-737340; Santa Cruz).

3D atomic force microscopy

Cells were incubated with 1.5 mg of Dynabeads Protein A (Invitrogen) with 10 µg of Fc-E-cadherin (Acro Biosystems). A tensile pulse of force (1 V) was applied to the cells, and bead displacement was monitored using live-cell imaging. A total of 90 beads adhered to cells were analyzed for all cell lines.

Immunofluorescence

Cells were fixed in 4% PFA in PBS, permeabilized in 0.5% Triton X-100 in universal buffer (UB; 150 mM NaCl, 50 mM Tris, pH 7.6, and 0.01% NaN_3), and washed in UB. Cells were blocked with 10% BSA in UB, incubated with a primary antibody, washed in UB, and then incubated with secondary antibody. F-actin was detected using phalloidin conjugated with Texas Red. E-cadherin was stained using mouse HECD-1 (Invitrogen) followed by FITC-conjugated goat anti-mouse IgG (H+L; Jackson ImmunoResearch Laboratories). To examine PAK2 and pPAK2, cells were fixed and permeabilized in a methanol/acetate solution and washed in PBS. Cells were blocked in 10% goat serum in PBS. PAK2 was visualized using mouse yPAK2 (E-9; Santa Cruz) followed by FITC-conjugated goat anti-mouse IgG (H+L; Jackson ImmunoResearch Laboratories). pPAK2 was stained using a rabbit phospho-specific PAK2 antibody (Cell Signaling) and Texas Red–conjugated donkey anti-rabbit IgG (H+L; Jackson ImmunoResearch Laboratories). Fluorescence images were captured using a confocal microscope (model LSM710; Zeiss) with a 40×/NA 1.4 oil objective at room temperature. DAPI, anti-mouse Alexa Fluor 488, anti-rabbit Alexa Fluor 488, anti-rabbit Alexa Fluor 594, and anti-mouse Alexa Fluor 594 fluorochromes were used. Images were acquired using Zeiss ZEN 2012 Digital Imaging acquisition software. Quantifications of fluorescence intensity at cell–cell junctions were made using ImageJ software (National Institutes of Health). 50 junctions were chosen at random and measured over at least five fields of view with the data analyzer blinded to image identity. Graphs depict the corrected fluorescence intensity of regions of interest. Data are represented as a box-and-whisker plot with 90th to 10th percentiles shown.

In vitro binding assays

Purified GST-PAK2 (Abcam), His-AMPK (Abcam), and His-Abl (MBL) were incubated in lysis buffer (20 mM Tris, pH 7.6, 150 mM NaCl, 0.1% NP-40, 2 mM $MgCl_2$, and 20 µg/ml aprotinin). PAK2 was recovered using glutathione-sepharose beads (Sigma) and resuspended in 2× sample buffer.

In vitro kinase assay

Purified GST-PAK2 and His-AMPK were incubated in in vitro kinase buffer (20 mM Pipes, pH 7.0, 20 µg aprotinin/ml, 10 mM $MnCl_2$, and 1 mM ATP). The reaction was terminated in 2× sample buffer.

In vitro cleavage assay

Purified GST-PAK2 was incubated with or without His-AMPK in the presence of purified, active caspase-3 (Abcam) in in vitro cleavage buffer (50 mM Hepes, 50 mM NaCl, 10 mM DTT, 1 mM EDTA, and 5% glycerol) at 4°C. The reaction was terminated in 2× Laemmli sample buffer.

Apoptosis assays

Cells were subjected to shear stress (200 rpm for 2 h) or left resting. To quantify apoptosis using annexin V staining, the cells were trypsinized, washed with PBS, and stained with APC-annexin V (556547; BD Biosciences). The cells were sorted for annexin V and Hoechst 33258 for cell death and cell viability on a BD Biosciences LSR II with UV instrument.

Glucose uptake assays

Glucose uptake was measured using a kit from Cayman Chemical (600470). 1.0 × 10^5 cells/well were plated in 24-well plates.

Cells were transferred to PBS, and 33 µg of 2-NBDG, a fluorescently tagged glucose derivative, was added. Shear stress was applied to the cells for 2 h, and then the cells recovered for 10 min. The cells were transferred to ice and lysed in 250 µl of 10 mM Tris, pH 7.4, 50 mM NaCl, 5 mM EDTA, 50 mM NaF, 1% Triton X-100, and protease inhibitors. The lysates were clarified by centrifugation at 12,000 rpm for 5 min at 4°C. The supernatant was collected, and an equal volume of Cell-Based Assay Buffer (10009322; Cayman Chemical) was added. 100 µl of the solution was loaded into a 96-well plate in triplicate, and the fluorescence at 485/535 nm was measured. The glucose uptake concentration was determined using a standard curve. Results are reported as micrograms per milliliter per 10^5 cells.

Statistics and reproducibility

Statistical differences were analyzed using two-tailed unpaired Student *t* tests. Experiments were done at least three independent times, and key findings were replicated by at least two authors.

Online supplemental material

The supplemental material contains a characterization of the process described in the article. Fig. S1 contains a characterization of PAK2 activation. Specifically, data are presented showing force induced PAK2 activation monitored by different phosphospecific antibodies and PAK2 activation in different cell lines. Additionally, data are presented showing the specificity of PAK2 activation as well as PAK2 localization to cell–cell, but not cell–matrix, adhesions. Fig. S2 contains in vitro data demonstrating direct binding between AMPK and Abl as well as AMPK-mediated phosphorylation of PAK2. Data are also presented showing the effects of AMPK on PAK2 cleavage and the effects of loss of PAK2 on Bad levels.

Acknowledgments

We thank G. DeWane and J. Bays at the University of Iowa for the generation of cell lines and preliminary studies related to this manuscript.

Research reported in this publication was supported by National Institute of General Medical Sciences (Award Number R01GM112805 to K.A. DeMali) and the National Cancer Institute of the National Institutes of Health (Award Number P30CA086862). Predoctoral fellowships from the National Institutes of Health (Award T32 GM067795) and the American Heart Association (18PRE33960274) support A.M. Salvi and H.K. Campbell, respectively. Work conducted with R. Superfine was supported by the National Institutes of Health through grant P41-EB002025-34.

The authors declare no competing financial interests.

H.K. Campbell designed and performed experiments, analyzed all the data, and helped write the manuscript. A.M. Salvi performed the immunofluorescence studies. T. O'Brien and R. Superfine designed and aided in adaptive stiffening experiments. K.A. DeMali helped with the experimental design, wrote the manuscript, and directed the project. All authors provided detailed comments.

Submitted: 20 July 2018
Revised: 29 January 2019
Accepted: 20 March 2019

References

Banko, M.R., J.J. Allen, B.E. Schaffer, E.W. Wilker, P. Tsou, J.L. White, J. Villén, B. Wang, S.R. Kim, K. Sakamoto, et al. 2011. Chemical genetic screen for AMPKα2 substrates uncovers a network of proteins involved in mitosis. *Mol. Cell.* 44:878–892. https://doi.org/10.1016/j.molcel.2011.11.005

Barry, A.K., H. Tabdili, I. Muhamed, J. Wu, N. Shashikanth, G.A. Gomez, A.S. Yap, C.J. Gottardi, J. de Rooij, N. Wang, and D.E. Leckband. 2014. α-catenin cytomechanics--role in cadherin-dependent adhesion and mechanotransduction. *J. Cell Sci.* 127:1779–1791. https://doi.org/10.1242/jcs.139014

Bays, J.L., X. Peng, C.E. Tolbert, C. Guilluy, A.E. Angell, Y. Pan, R. Superfine, K. Burridge, and K.A. DeMali. 2014. Vinculin phosphorylation differentially regulates mechanotransduction at cell-cell and cell-matrix adhesions. *J. Cell Biol.* 205:251–263. https://doi.org/10.1083/jcb.201309092

Bays, J.L., H.K. Campbell, C. Heidema, M. Sebbagh, and K.A. DeMali. 2017. Linking E-cadherin mechanotransduction to cell metabolism through force-mediated activation of AMPK. *Nat. Cell Biol.* 19:724–731. https://doi.org/10.1038/ncb3537

Bertocchi, C., Y. Wang, A. Ravasio, Y. Hara, Y. Wu, T. Sailov, M.A. Baird, M. W. Davidson, R. Zaidel-Bar, Y. Toyama, et al. 2017. Nanoscale architecture of cadherin-based cell adhesions. *Nat. Cell Biol.* 19:28–37. https://doi.org/10.1038/ncb3456

Bilek, A.M., K.C. Dee, and D.P. Gaver III. 2003. Mechanisms of surface-tension-induced epithelial cell damage in a model of pulmonary airway reopening. *J. Appl. Physiol.* 94:770–783. https://doi.org/10.1152/japplphysiol.00764.2002

Button, B.M., and B. Button. 2013. Structure and function of the mucus clearance system of the lung. *Cold Spring Harb. Perspect. Med.* 3:a009720. https://doi.org/10.1101/cshperspect.a009720

Byers, S.W., C.L. Sommers, B. Hoxter, A.M. Mercurio, and A. Tozeren. 1995. Role of E-cadherin in the response of tumor cell aggregates to lymphatic, venous and arterial flow: measurement of cell-cell adhesion strength. *J. Cell Sci.* 108:2053–2064.

Cohen, L., X. e, J. Tarsi, T. Ramkumar, T.K. Horiuchi, R. Cochran, S. DeMartino, K.B. Schechtman, I. Hussain, M.J. Holtzman, and M. Castro. NHLBI Severe Asthma Research Program (SARP). 2007. Epithelial cell proliferation contributes to airway remodeling in severe asthma. *Am. J. Respir. Crit. Care Med.* 176:138–145. https://doi.org/10.1164/rccm.200607-1062OC

Collins, C., C. Guilluy, C. Welch, E.T. O'Brien, K. Hahn, R. Superfine, K. Burridge, and E. Tzima. 2012. Localized tensional forces on PECAM-1 elicit a global mechanotransduction response via the integrin-RhoA pathway. *Curr. Biol.* 22:2087–2094. https://doi.org/10.1016/j.cub.2012.08.051

Coniglio, S.J., S. Zavarella, and M.H. Symons. 2008. Pak1 and Pak2 mediate tumor cell invasion through distinct signaling mechanisms. *Mol. Cell. Biol.* 28:4162–4172. https://doi.org/10.1128/MCB.01532-07

Delorme-Walker, V.D., J.R. Peterson, J. Chernoff, C.M. Waterman, G. Danuser, C. DerMardirossian, and G.M. Bokoch. 2011. Pak1 regulates focal adhesion strength, myosin IIA distribution, and actin dynamics to optimize cell migration. *J. Cell Biol.* 193:1289–1303. https://doi.org/10.1083/jcb.201010059

Flitney, E.W., E.R. Kuczmarski, S.A. Adam, and R.D. Goldman. 2009. Insights into the mechanical properties of epithelial cells: the effects of shear stress on the assembly and remodeling of keratin intermediate filaments. *FASEB J.* 23:2110–2119. https://doi.org/10.1096/fj.08-124453

Frank, S.R., J.H. Bell, M. Frödin, and S.H. Hansen. 2012. A βPIX-PAK2 complex confers protection against Scrib-dependent and cadherin-mediated apoptosis. *Curr. Biol.* 22:1747–1754. https://doi.org/10.1016/j.cub.2012.07.011

Fuhrmann, A., A. Banisadr, P. Beri, T.D. Tlsty, and A.J. Engler. 2017. Metastatic State of Cancer Cells May Be Indicated by Adhesion Strength. *Biophys. J.* 112:736–745. https://doi.org/10.1016/j.bpj.2016.12.038

Goeckeler, Z.M., R.A. Masaracchia, Q. Zeng, T.L. Chew, P. Gallagher, and R.B. Wysolmerski. 2000. Phosphorylation of myosin light chain kinase by p21-activated kinase PAK2. *J. Biol. Chem.* 275:18366–18374. https://doi.org/10.1074/jbc.M001339200

Guilluy, C., V. Swaminathan, R. Garcia-Mata, E.T. O'Brien, R. Superfine, and K. Burridge. 2011. The Rho GEFs LARG and GEF-H1 regulate the

mechanical response to force on integrins. *Nat. Cell Biol.* 13:722–727. https://doi.org/10.1038/ncb2254

Huo, Y., T. Wischgoll, and G.S. Kassab. 2007. Flow patterns in three-dimensional porcine epicardial coronary arterial tree. *Am. J. Physiol. Heart Circ. Physiol.* 293:H2959–H2970. https://doi.org/10.1152/ajpheart.00586.2007

Jakobi, R., E. Moertl, and M.A. Koeppel. 2001. p21-activated protein kinase gamma-PAK suppresses programmed cell death of BALB3T3 fibroblasts. *J. Biol. Chem.* 276:16624–16634. https://doi.org/10.1074/jbc.M007753200

Jakobi, R., C.C. McCarthy, M.A. Koeppel, and D.K. Stringer. 2003. Caspase-activated PAK-2 is regulated by subcellular targeting and proteasomal degradation. *J. Biol. Chem.* 278:38675–38685. https://doi.org/10.1074/jbc.M306494200

Jung, J.H., A.M. Pendergast, P.A. Zipfel, and J.A. Traugh. 2008. Phosphorylation of c-Abl by protein kinase Pak2 regulates differential binding of ABI2 and CRK. *Biochemistry.* 47:1094–1104. https://doi.org/10.1021/bi701533j

Kim, T.J., S. Zheng, J. Sun, I. Muhamed, J. Wu, L. Lei, X. Kong, D.E. Leckband, and Y. Wang. 2015. Dynamic visualization of α-catenin reveals rapid, reversible conformation switching between tension states. *Curr. Biol.* 25:218–224. https://doi.org/10.1016/j.cub.2014.11.017

Li, Y.S., J.H. Haga, and S. Chien. 2005. Molecular basis of the effects of shear stress on vascular endothelial cells. *J. Biomech.* 38:1949–1971. https://doi.org/10.1016/j.jbiomech.2004.09.030

Luo, S., and D.C. Rubinsztein. 2009. Huntingtin promotes cell survival by preventing Pak2 cleavage. *J. Cell Sci.* 122:875–885. https://doi.org/10.1242/jcs.050013

Mahto, S.K., J. Tenenbaum-Katan, A. Greenblum, B. Rothen-Rutishauser, and J. Sznitman. 2014. Microfluidic shear stress-regulated surfactant secretion in alveolar epithelial type II cells in vitro. *Am. J. Physiol. Lung Cell. Mol. Physiol.* 306:L672–L683. https://doi.org/10.1152/ajplung.00106.2013

Maiers, J.L., X. Peng, A.S. Fanning, and K.A. DeMali. 2013. ZO-1 recruitment to α-catenin--a novel mechanism for coupling the assembly of tight junctions to adherens junctions. *J. Cell Sci.* 126:3904–3915. https://doi.org/10.1242/jcs.126565

Manser, E., H.Y. Huang, T.H. Loo, X.Q. Chen, J.M. Dong, T. Leung, and L. Lim. 1997. Expression of constitutively active alpha-PAK reveals effects of the kinase on actin and focal complexes. *Mol. Cell. Biol.* 17:1129–1143. https://doi.org/10.1128/MCB.17.3.1129

Marlin, J.W., A. Eaton, G.T. Montano, Y.W. Chang, and R. Jakobi. 2009. Elevated p21-activated kinase 2 activity results in anchorage-independent growth and resistance to anticancer drug-induced cell death. *Neoplasia.* 11:286–297. https://doi.org/10.1593/neo.81446

Mitchell, M.J., C. Denais, M.F. Chan, Z. Wang, J. Lammerding, and M.R. King. 2015. Lamin A/C deficiency reduces circulating tumor cell resistance to fluid shear stress. *Am. J. Physiol. Cell Physiol.* 309:C736–C746. https://doi.org/10.1152/ajpcell.00050.2015

Nayal, A., D.J. Webb, C.M. Brown, E.M. Schaefer, M. Vicente-Manzanares, and A.R. Horwitz. 2006. Paxillin phosphorylation at Ser273 localizes a GIT1-PIX-PAK complex and regulates adhesion and protrusion dynamics. *J. Cell Biol.* 173:587–589. https://doi.org/10.1083/jcb.200509075

Neto, A.S., S.N. Hemmes, C.S. Barbas, M. Beiderlinden, A. Fernandez-Bustamante, E. Futier, O. Gajic, M.R. El-Tahan, A.A. Ghamdi, E. Günay, et al.; PROVE Network Investigators. 2016. Association between driving pressure and development of postoperative pulmonary complications in patients undergoing mechanical ventilation for general anaesthesia: a meta-analysis of individual patient data. *Lancet Respir. Med.* 4:272–280. https://doi.org/10.1016/S2213-2600(16)00057-6

Paszek, M.J., N. Zahir, K.R. Johnson, J.N. Lakins, G.I. Rozenberg, A. Gefen, C.A. Reinhart-King, S.S. Margulies, M. Dembo, D. Boettiger, et al. 2005. Tensional homeostasis and the malignant phenotype. *Cancer Cell.* 8:241–254. https://doi.org/10.1016/j.ccr.2005.08.010

Ridge, K.M., L. Linz, F.W. Flitney, E.R. Kuczmarski, Y.H. Chou, M.B. Omary, J.I. Sznajder, and R.D. Goldman. 2005. Keratin 8 phosphorylation by protein kinase C delta regulates shear stress-mediated disassembly of keratin intermediate filaments in alveolar epithelial cells. *J. Biol. Chem.* 280:30400–30405. https://doi.org/10.1074/jbc.M504239200

Roig, J., P.T. Tuazon, P.A. Zipfel, A.M. Pendergast, and J.A. Traugh. 2000. Functional interaction between c-Abl and the p21-activated protein kinase gamma-PAK. *Proc. Natl. Acad. Sci. USA.* 97:14346–14351. https://doi.org/10.1073/pnas.97.26.14346

Sells, M.A., J.T. Boyd, and J. Chernoff. 1999. p21-activated kinase 1 (Pak1) regulates cell motility in mammalian fibroblasts. *J. Cell Biol.* 145:837–849. https://doi.org/10.1083/jcb.145.4.837

Sells, M.A., A. Pfaff, and J. Chernoff. 2000. Temporal and spatial distribution of activated Pak1 in fibroblasts. *J. Cell Biol.* 151:1449–1458. https://doi.org/10.1083/jcb.151.7.1449

Slutsky, A.S., and V.M. Ranieri. 2013. Ventilator-induced lung injury. *N. Engl. J. Med.* 369:2126–2136. https://doi.org/10.1056/NEJMra1208707

Tözeren, A., H.K. Kleinman, D.S. Grant, D. Morales, A.M. Mercurio, and S.W. Byers. 1995. E-selectin-mediated dynamic interactions of breast- and colon-cancer cells with endothelial-cell monolayers. *Int. J. Cancer.* 60:426–431. https://doi.org/10.1002/ijc.2910600326

Tzima, E., M. Irani-Tehrani, W.B. Kiosses, E. Dejana, D.A. Schultz, B. Engelhardt, G. Cao, H. DeLisser, and M.A. Schwartz. 2005. A mechanosensory complex that mediates the endothelial cell response to fluid shear stress. *Nature.* 437:426–431. https://doi.org/10.1038/nature03952

Walter, B.N., Z. Huang, R. Jakobi, P.T. Tuazon, E.S. Alnemri, G. Litwack, and J.A. Traugh. 1998. Cleavage and activation of p21-activated protein kinase gamma-PAK by CPP32 (caspase 3). Effects of autophosphorylation on activity. *J. Biol. Chem.* 273:28733–28739. https://doi.org/10.1074/jbc.273.44.28733

Wang, R.L., K. Xu, K.L. Yu, X. Tang, and H. Xie. 2012. Effects of dynamic ventilatory factors on ventilator-induced lung injury in acute respiratory distress syndrome dogs. *World J. Emerg. Med.* 3:287–293. https://doi.org/10.5847/wjem.j.issn.1920-8642.2012.04.009

Yoon, K.H., M. Yoon, R.D. Moir, S. Khuon, F.W. Flitney, and R.D. Goldman. 2001. Insights into the dynamic properties of keratin intermediate filaments in living epithelial cells. *J. Cell Biol.* 153:503–516. https://doi.org/10.1083/jcb.153.3.503